

Polaron Problem by Diagrammatic Quantum Monte Carlo

Nikolai V. Prokof'ev and Boris V. Svistunov

Russian Research Center, "Kurchatov Institute," 123182 Moscow, Russia

(Received 8 April 1998)

We present a numerical solution of the polaron problem by a novel Monte Carlo method. Starting from a conventional diagrammatic expansion for the polaron Green function $G(\mathbf{k}, \tau)$, we construct a process which generates continuous random variables \mathbf{k} and τ , with a distribution function coinciding exactly with $G(\mathbf{k}, \tau)$. The polaron spectrum is extracted from the asymptotic behavior of the Green function. We compare our results for the polaron energy with the variational treatment of Feynman, and present an accurate dispersion curve which features an end point at finite momentum. [S0031-9007(98)07144-0]

PACS numbers: 71.38.+i, 02.70.Lq, 05.20.-y

The polaron problem has a long history starting from the work of Landau [1]. In its most general form, it asks what happens to a particle coupled to an environment, and what are the properties of the resulting object, called a polaron, which consists of the bare particle dressed by environmental excitations. This problem arises over and over again because of its fundamental importance both for high-energy and for condensed matter physics, and also because the notion of what we call "particles" becomes more diverse as new kinds of environment appear (e.g., hole excitations in spin environments). In this paper we describe how the polaron problem can be solved numerically without systematic errors using a diagrammatic Monte Carlo (MC) method and present results for the notorious Fröhlich model (see, e.g., Refs. [2,3]). First, we explain in detail how this model fits into our general MC scheme [4,5] dealing with distribution functions of continuous variables. We then describe the procedure of extracting the polaron spectrum, $E(k)$, from the asymptotic decay of the Green function. Although for small electron-phonon coupling the polaron energy E_0 and the effective mass m_* at the bottom of the polaron band are rather well given by perturbation theory, the lowest order perturbation theory fails to describe the spectrum near the threshold $E(k) - E_0 \approx \omega_p$, where ω_p is the frequency of the optical phonon. In fact, the threshold features an end point [6,7]

$$E(k) = E_0 + \omega_p - \frac{(k - k_c)^2}{2m_c} \quad (k < k_c), \quad (1)$$

analogous to the end point of the excitation spectrum in ^4He described by Pitaevskii [8]. Our numerical data unambiguously confirm this conclusion.

We start by considering the underlying mathematics. Suppose that for a certain random variable (set of variables), y , the distribution function $Q(y)$ is given in terms of a series of integrals with an ever increasing number of integration variables,

$$Q(y) = \sum_{m=0}^{\infty} \sum_{\xi_m} \int dx_1 \cdots dx_m F(\xi_m, y, x_1, \dots, x_m). \quad (2)$$

Here ξ_m indexes different terms of the same order m . The term $m = 0$ is understood as a certain function of y . In Refs. [4,5] it was shown how to arrange a Metropolis-type stochastic process simulating the distribution $Q(y)$ exactly. The process has much in common with the MC simulation of a distribution given by a multidimensional integral. Nevertheless, the crucial difference is associated with the fact that the integration multiplicity in the expansion Eq. (2) is varying.

The projection onto the polaron problem is as follows. Let us interpret the Matsubara (imaginary time) Green function of the polaron in the momentum-time representation, $G(\mathbf{k}, \tau)$, as the distribution function for the random variables \mathbf{k} and τ . We thus identify G with Q and (\mathbf{k}, τ) with y . Equation (2) is then identified with the diagrammatic expansion of $G(\mathbf{k}, \tau)$ in terms of free-electron and phonon propagators within the framework of a conventional Matsubara technique at $T = 0$. Then, the variables x_1, x_2, \dots, x_m are the internal times and independent momenta of the diagram ξ_m . A typical diagram is presented in Fig. 1. Solid lines denote the free-electron propagators, $G^{(0)}(\mathbf{p}, \tau_2 - \tau_1) = e^{-(p^2/2 - \mu)(\tau_2 - \tau_1)}$, where μ is the chemical potential (Planck's constant and the electron mass are set equal to unity). Dashed lines and points stand for phonon propagators, $D(\mathbf{q}, \tau_2 - \tau_1)$, and electron-phonon coupling vertices, $V(\mathbf{q})$, respectively. We fix the left end of the diagram at the origin of imaginary time, ascribing thus the time τ to the right end.

In this paper we confine ourselves to the Fröhlich model [2] where phonons are considered to be dispersionless,

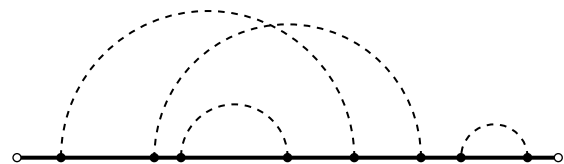


FIG. 1. A typical diagram contributing to the polaron Green function.

and the electron-phonon coupling has the form,

$$H_{e-ph} = \sum_{\mathbf{k}, \mathbf{q}} V(\mathbf{q}) (b_{\mathbf{q}}^{\dagger} - b_{-\mathbf{q}}) a_{\mathbf{k}-\mathbf{q}}^{\dagger} a_{\mathbf{k}}, \quad (3)$$

$$V(\mathbf{q}) = i(2\sqrt{2} \alpha \pi)^{1/2} \frac{1}{q}. \quad (4)$$

In Eq. (3) $a_{\mathbf{k}}$ and $b_{\mathbf{q}}$ are the annihilation operators for the electron with momentum \mathbf{k} and for the phonon with momentum \mathbf{q} , respectively; α is a dimensionless coupling constant. In the Fröhlich model the phonon propagator is independent of momentum: $D(\mathbf{q}, \tau_2 - \tau_1) = \exp[-\omega_p(\tau_2 - \tau_1)]$. It is convenient, however, to attribute the vertex factors to the dashed lines, so that a dashed line with momentum \mathbf{q} contributes the factor $\tilde{D}(\mathbf{q}, \tau_2 - \tau_1) = |V(\mathbf{q})|^2 D(\tau_2 - \tau_1)$ to the diagram. The function F is thus expressed as a product of $G^{(0)}$'s and \tilde{D} 's, in accordance with the standard diagrammatic rules.

Simulating the distribution $Q(y)$ is the process of sequential stochastic generation of diagrams, such as in Fig. 1, with certain fixed times and momenta. The MC process consists of a number of elementary updates falling into two qualitatively different classes: (I) those which do not change the type of the diagram (change the values of arguments in F , but not the function itself), and (II) those which do change the structure of the diagram. The updates of class I are rather straightforward, being identical to those of simulating continuous distribution corresponding to the given function F . In this paper we use only one update of this type, namely, shifting in time the right end of the diagram in Fig. 1.

In the heart of the method are updates of type II. The generic rules for constructing them are as follows [5]. Let the update \mathcal{A} transform a diagram $F(\xi_m, y, x_1, \dots, x_m)$ into $F(\xi_{m+n}, y, x_1, \dots, x_m, x_{m+1}, \dots, x_{m+n})$, and, correspondingly, its counterpart \mathcal{B} performs the inverse transformation. For n new variables we introduce the vector notation: $\vec{x} = \{x_{m+1}, x_{m+2}, \dots, x_{m+n}\}$. The update procedure \mathcal{A} involves two steps. First, it *proposes* a change, selecting a new type of diagram, ξ_{m+n} , and a particular value of \vec{x} . The vector \vec{x} is selected with a certain normalized distribution function $W(\vec{x})$. There are no requirements strictly fixing the form of $W(\vec{x})$, but to render the algorithm most efficient, it is desirable that $W(\vec{x})$ be chosen as close as possible to $F(\xi_{m+n}, y, \vec{x})$. Upon proposing the modification, the update is accepted with the probability $P_{\text{acc}}(\vec{x})$, or rejected. The update \mathcal{B} , removing variables \vec{x} , is accepted with probability $P_{\text{rem}}(\vec{x})$. For the pair of complementary updates to be balanced, the following Metropolis-like prescription should be fulfilled [5]:

$$P_{\text{acc}}(\vec{x}) = \begin{cases} R(\vec{x})/W(\vec{x}), & \text{if } R(\vec{x}) < W(\vec{x}), \\ 1, & \text{otherwise,} \end{cases} \quad (5)$$

$$P_{\text{rem}}(\vec{x}) = \begin{cases} W(\vec{x})/R(\vec{x}) & \text{if } R(\vec{x}) > W(\vec{x}), \\ 1, & \text{otherwise,} \end{cases} \quad (6)$$

where

$$R(\vec{x}) = \frac{p_{\mathcal{B}}}{p_{\mathcal{A}}} \frac{F(\xi_{m+n}, y, x_1, \dots, x_m, \vec{x})}{F(\xi_m, y, x_1, \dots, x_m)} \quad (7)$$

and $p_{\mathcal{A}}$ and $p_{\mathcal{B}}$ are the probabilities of selecting updates \mathcal{A} and \mathcal{B} , which, in principle, may differ. To solve the polaron problem and account for any possible diagram it is sufficient to have only one pair of complementary updates of type II: the update \mathcal{A} adding a new phonon propagator to the diagram and its counterpart \mathcal{B} removing one phonon propagator from the diagram.

Consider the algorithm for \mathcal{A} . First we select the position τ_1 for the left-hand end of the extra phonon propagator. This is done by choosing at random (with equal probabilities) one of the free-electron propagators and by taking for τ_1 any time (with equal probability density) within this propagator. Second we select the position τ_2 for the right-hand end of the phonon propagator, in accordance with the distribution function $\propto \exp[-\omega_p(\tau_2 - \tau_1)]$. After that, we select the momentum for this propagator, using the distribution $\propto (1 + q/q_0)^{-2}$, where $q_0^2/2 = \omega_p$. Now the proposing stage is completed, and we are ready to perform an accept (reject) step, following the above prescription, Eq. (5). The corresponding function $W(\vec{x})$ ($\vec{x} \equiv \{\tau_1, \tau_2, \mathbf{q}\}$) reads

$$W(\vec{x}) \propto \frac{1}{\tau_0} \frac{1}{(1 + q/q_0)^2} e^{-\omega_p(\tau_2 - \tau_1)}, \quad (8)$$

where τ_0 is the length of the free-electron propagator, and where the point τ_1 is selected. Apart from the factor $p_{\mathcal{B}}/p_{\mathcal{A}}$, the ratio (7) is now completely defined.

The algorithm for \mathcal{B} is to select at random (with equal probabilities) some phonon propagator and with the probabilities given in Eqs. (6)–(8) to remove it.

We now define the ratio $p_{\mathcal{B}}/p_{\mathcal{A}}$. The simplest choice would be to have equal probabilities for selecting the creation and annihilation procedures at each MC step. It might seem that this leads to $p_{\mathcal{B}}/p_{\mathcal{A}} = 1$, but this is not true. When we select an electron propagator to decide about point τ_1 , we have N_e equal chances, where N_e is the number of free-electron propagators in the diagram being modified [denominator of Eq. (7)]. When we select a phonon propagator to be removed, we have N_{ph} equal chances, where N_{ph} is the number of phonon propagators in the diagram [numerator of Eq. (7)]. N_e and N_{ph} are straightforwardly related to each other,

$$N_{\text{ph}} = (N_e + 1)/2. \quad (9)$$

We thus get

$$\frac{p_{\mathcal{B}}}{p_{\mathcal{A}}} = \frac{N_e + 1}{2N_e} = \frac{N_{\text{ph}}}{2N_{\text{ph}} - 1}. \quad (10)$$

As for the updates of type I, these may include (i) the selection of time τ anywhere on the interval $(\tau_{2N_{\text{ph}}}, \infty)$ according to the simple exponential distribution of $G^{(0)}(\mathbf{k}, \tau - \tau_{2N_{\text{ph}}})$ [obviously, the role of the chemical potential is to make this distribution normalizable; in fact, we use μ as a tuning parameter to probe different

time scales since the typical length of the diagram in time is controlled by the inverse of $E(k) - \mu$, and (ii) the change of the diagram momentum from \mathbf{k} to $\mathbf{k} + \mathbf{p}$ according to the distribution function $\exp[-(\bar{\mathbf{k}} + \mathbf{p})^2 \tau / 2m]$, where $\bar{\mathbf{k}}$ is the average electron momentum of the diagram, i.e., $\bar{\mathbf{k}} = \tau^{-1} \int_0^\tau d\tau' \mathbf{k}(\tau')$. We find it more efficient, however, to select the incoming momentum at will and keep it fixed, since in this case we collect all the statistics for the value of k we are interested in, instead of spreading it over the entire k histogram.

As mentioned already the W distribution function according to which one is selecting the new diagram variables is arbitrary, but the best possible choice would be $W_{\text{best}}(\vec{x}) \propto \bar{D}(\mathbf{q}, \tau_2 - \tau_1) \exp\{-\int_{\tau_1}^{\tau_2} d\tau [(\mathbf{p}(\tau) - \mathbf{q})^2 - \mathbf{p}^2(\tau)]/2\}$, so that the accept (reject) probabilities in Eqs. (5) and (6) are independent of \vec{x} . However, it is not known in the general case how to map the homogeneous (on the unit interval) multidimensional distribution of random numbers r_1, \dots, r_4 to arbitrary W . Such a mapping is easy if $W = \prod_{i=1}^4 W_i(x_i)$ factorizes [as in Eq. (8)], and one simply has to choose the functional form which allows an analytic (i.e., very fast) solution of one-dimensional equations $\int_{a_i}^{x_i} dy W_i(y) = r_i$, where $\{W_i\}$ are defined on intervals (a_i, b_i) , and their product is as close as possible to W_{best} . We believe this is the most efficient way of summing the diagrammatic series for G .

In Fig. 2 we show the typical data for the polaron Green function. Following Ref. [3], we use energy units such that $\omega_p = 1$. After an initial drop at short times [the overall normalization of the Green function is established from $G(k, \tau \rightarrow 0) \rightarrow G^{(0)}(k, 0) = 1$] we observe a pure exponential decay of $G(\mathbf{k}, \tau)$ at longer times [provided we are below the threshold of Cherenkov radiation, $E(k) - E_0 < \omega_p$, so that the polaron state is stable]. From the exponential asymptotic of the Green function we readily extract the polaron energy,

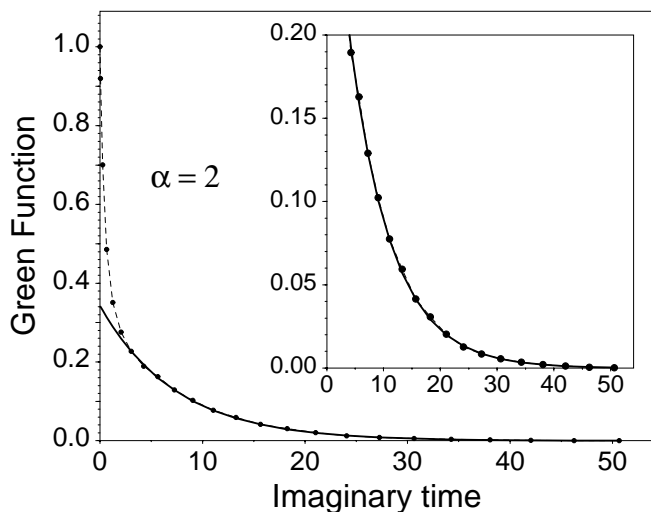


FIG. 2. Polaron Green function $G(k = 0, \tau)$ for $\alpha = 2$ and $\mu = -2.2$. The solid line is the exponential fit.

$$G(k, \tau \gg \omega_p^{-1}) \rightarrow Z_k \exp\{-[E(k) - \mu]\tau\}. \quad (11)$$

By fine-tuning the chemical potential close to $E(k)$ we may extend the time scale for $G(k, \tau)$ which is given by $1/[E(k) - \mu]$. Typically, we had reliable statistics on the time scale of the order of $100/\omega_p$ and were thus able to deduce the polaron energy to accuracy better than $0.01 \omega_p$. Apart from the polaron energy, the asymptotic behavior of the Green function (11) gives us one more important physical characteristic of the polaron, the factor Z_k , which shows the fraction of the bare-electron state in the true eigenstate of the polaron

$$Z_k = |\langle \text{free particle}_k | \text{polaron}_k \rangle|^2. \quad (12)$$

In Fig. 3 we present our results for the bottom of the band E_0 as a function of the coupling strength α in the most interesting intermediate region $0 < \alpha \leq 6$. As expected, our data are below the solid line which gives the upper bound for E_0 (known to be the lowest ever obtained for this problem) as derived from Feynman's variational treatment [3]. We note the remarkable accuracy of Feynman's approach to the polaron energy.

However, the most interesting and instructive data are for the polaron spectrum at relatively large k . The perturbation theory result for the dispersion law, $E(k) \approx k^2/2 - \alpha(\sqrt{2}/k) \sin^{-1}(k/\sqrt{2})$ (the solid line in Fig. 4), clearly demonstrates that the first-order correction is singular near the optical phonon emission threshold and even develops an unphysical maximum [by assumption, the threshold point was defined as $E(k_c) = E_0 + \omega_p$; the maximum on the dispersion curve at $k < k_c$ is in

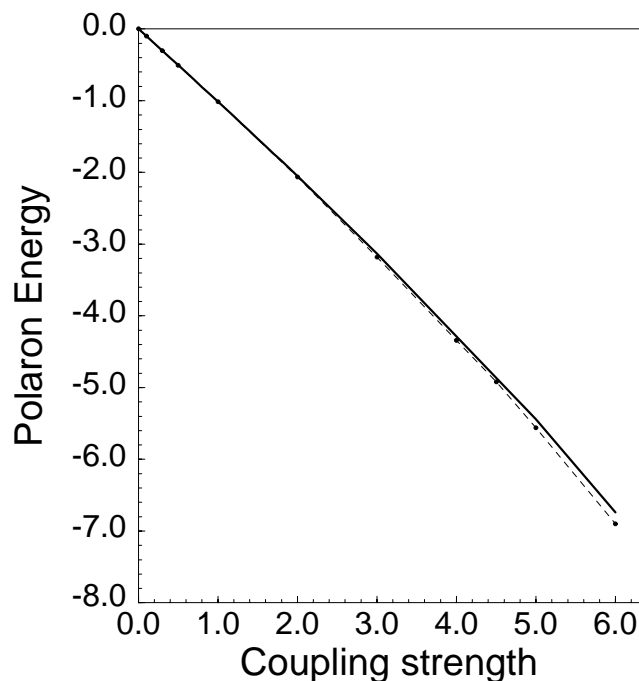


FIG. 3. Polaron energy E_0 as a function of the coupling strength. The solid line is Feynman's variational result.

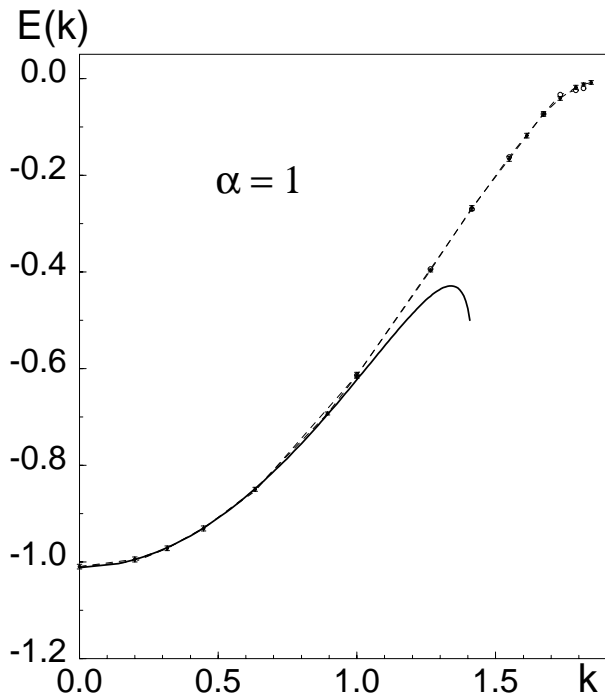


FIG. 4. Polaron dispersion law for $\alpha = 1$. The solid line is the first-order perturbation theory result.

contradiction with this assumption]. One is bound to admit then that near the threshold the lowest order perturbation theory fails at any α , because of the singular phonon density of states, which is δ functional when one ignores the curvature of the phonon dispersion law $\omega_p(q) \approx \omega_p = \text{const}$ [6,7]. The formalism dealing with such cases was developed by Pitaevskii [8] for the end point in ^4He (a similar approach based on the Tamm-Dankoff approximation was suggested in Refs. [2,9] and developed further in [6,7]). By applying it to the Fröhlich model we arrive at the following equation for the dispersion law:

$$\tilde{\omega} - a(k - k_c) + b\tilde{\omega} \int \frac{dx}{x^2 - \tilde{\omega}} + R(k - k_c, \tilde{\omega}) = 0, \quad (13)$$

where $\tilde{\omega} \equiv \omega - (E_0 + \omega_p)$, R is a smooth function of $k - k_c$ and $\tilde{\omega}$, a , and b are some coefficients depending on α and k_c . This equation features an end point at k_c , with the parabolic dependence, Eq. (1), at $k < k_c$. The MC data obtained for $\alpha = 1$ are shown in Fig. 4. We see how an almost perfect agreement with the perturbation theory for the band bottom transforms into nonperturbative behavior near k_c predicted by Eq. (1).

Apparently, the end point is an artifact of the dispersionless phonon spectrum. With the nonzero curvature of $\omega_p(q)$ taken into account, the end point will transform into a sharp crossover from zero to finite damping

of the polaron state. We estimate the crossover region as $\Delta k/k_c \sim \sqrt{m/M}$, where M is the mass of the host-lattice atoms.

In summary, we have presented the numerical solution of the polaron problem by our diagrammatic quantum MC method, which directly simulates the polaron Green function in the 4D momentum-time continuum. This approach applies to any model dealing with 1 (few) degree of freedom, either continuous or discrete, coupled to the thermal bath. The series of the form of Eq. (2) also naturally represents the partition function in the interaction picture [4,5], and this approach was used recently to calculate the smearing of the Coulomb staircase in quantum dots [10]. More generally, diagrammatic MC solves any problem which can be reduced to a convergent series (2). (It may happen that perturbative expansion forms an asymptotic series; in which case the above approach does not work, e.g., an expansion in α for $H = p^2/2m + m\omega_0^2 x^2/2 + \alpha x^4$.) The efficiency, however, severely depends on the sign problem, and the convergence becomes very poor if F functions are not positive definite. The sign problem may originate from the particle statistics or from the alternating sign of matrix elements contributing to different diagrams. It is thus of crucial importance to work in the representation in which the sign problem is absent.

We thank N. Nagaosa, A. Furusaki, and Yu. Kagan for many fruitful discussions. We also mention that the polaron problem was brought to our attention and suggested for solution by N. Nagaosa. We acknowledge the support from the Russian Foundation for Basic Research (Grant No. 98-02-16262).

-
- [1] L. D. Landau, *Sov. Phys.* **3**, 664 (1933).
 - [2] H. Fröhlich, H. Pelzer, and S. Zienau, *Philos. Mag.* **41**, 221 (1950).
 - [3] R. P. Feynman, *Statistical Mechanics* (Benjamin, Reading, 1972); see also R. P. Feynman, *Phys. Rev.* **97**, 660 (1955); T. D. Schultz, *Phys. Rev.* **116**, 526 (1959).
 - [4] N. V. Prokof'ev, B. V. Svistunov, and I. S. Tupitsyn, *Pis'ma Zh. Eksp. Teor. Fiz.* **64**, 853 (1996) [*Sov. Phys. JETP Lett.* **64**, 911 (1996)].
 - [5] N. V. Prokof'ev, B. V. Svistunov, and I. S. Tupitsyn, *Zh. Eksp. Teor. Fiz.* **114**, 570 (1998) [*Sov. Phys. JETP* (to be published)].
 - [6] G. D. Whitfield and R. Puff, in *Polarons and Excitons*, edited by C. G. Kuper and G. D. Whitfield (Plenum, New York, 1962), p. 171; *Phys. Rev.* **139**, A338 (1965).
 - [7] D. M. Larsen, *Phys. Rev.* **144**, 697 (1966).
 - [8] L. P. Pitaevskii, *Zh. Eksp. Teor. Fiz.* **36**, 1168 (1959).
 - [9] D. Pines, in *Polarons and Excitons*, edited by C. G. Kuper and G. D. Whitfield (Plenum, New York, 1962), p. 155.
 - [10] G. Göppert, H. Grabert, N. Prokof'ev, and B. V. Svistunov, *Phys. Rev. Lett.* (to be published).